Springer

KSME

Journal of Mechanical Science and Technology 30 (2) (2016) 567~574
www.springerlink.com/content/1738-494x(Print)/1976-3824(Online)
DOI 10.1007/s12206-016-0110-0

Application of different surrogate models on the optimization of centrifugal pump †

Wenjie Wang[1], Ji Pei[1,*], Shouqi Yuan[1], Jinfeng Zhang[1], Jianping Yuan[1] and Changzheng Xu[2]

[1]*National Research Center of Pumps, Jiangsu University, Zhenjiang, 212013, China*
[2]*Yixing Unite Machinery Co. Ltd., Wuxi, 214205, China*

(Manuscript Received June 2, 2015; Revised August 16, 2015; Accepted August 20, 2015)

Abstract

An optimization process for impellers was carried out based on numerical simulation, Latin hypercube sampling (LHS), surrogate model and Genetic algorithm (GA) to improve the efficiency of residual heat removal pump. The commercial software ANSYS CFX 14.5 was utilized to solve the Reynolds-averaged Navier-Stokes equations by using the Shear stress transport turbulence model. The impeller blade parameters, which contain the blade inlet incidence angle $\Delta\beta$, blade wrap angle φ, and blade outlet angle β_2, were designed by random sample points according to the LHS method. The efficiency predicted under the design flow rate was selected as the objective function. The best combination of parameters was obtained by calculating the surrogate model with the GA. Meanwhile, the prediction accuracies of three surrogate models, namely, Response surface model (RSM), Kriging model, and Radial basis neural network (RBNN), were compared. Results showed that the calculated findings agree with the experimental performance results of the original pump. The RSF model predicted the highest efficiency, while the RBNN had the highest prediction accuracy. Compared with the simulated efficiency of the original pump, the optimization increased efficiency by 8.34% under the design point. Finally, the internal flow fields were analyzed to understand the mechanism of efficiency improvement. The optimization process, including the comparison of the surrogate models, can provide reference for the optimization design of other pumps.

Keywords: Genetic algorithm; Impeller; Numerical simulation; Latin hypercube sampling; Optimization; Surrogate model

1. Introduction

In recent years, nuclear power has drawn increasing attention because of its high efficiency and low pollution. Thus, a rising number of nuclear power stations are being developed. The safety of nuclear station operations is mainly guaranteed by the residual heat removal system (Fig. 1). Residual heat removal pumps (RHRP) are operated when the nuclear main pump stops working and the nuclear station needs to be maintained [1].

Performance improvement has been investigated in turbomachinery for many years, and optimization methods have been proposed, such as Taguchi method, response surface methodology, artificial neural network, and surrogate model. The optimization algorithm is also developed to improve accuracy and reduce time and computational expense. Singh et al. [2] compared the Taguchi method and the Genetic algorithm (GA) to optimize pump performance and found that the former was the better choice for improving pump performance variables with multiple quality characteristics. Zhou et al. [3] used the numerical simulation and orthogonal experimental method to investigate the importance level of the main parameters of the impeller on pump performance and also obtained the best combination of parameters. Lian et al. [4] integrated the experiment design, Response surface model (RSM), GA, and Computational fluid dynamics (CFD) to redesign a single-stage pump, a two-stage turbo pump, and the NASA rotor67. The performance was improved and the computational cost was reduced. Yang et al. [5] applied the 3D inverse design method, CFD, response surface method, and the Multi-objective genetic algorithm (MGA) to redesign the pump-turbine. Wang et al. [6] developed an optimization method based on experimental design theory and response surface method to optimize a single-suction centrifugal pump and improve the performance of the optimal pump. Zhang et al. [7] applied the partial differential equation method to parametric design impeller and hypersurface response model to optimize the impeller. Zhang et al. [8] proposed a multi-objective optimization method for a double suction centrifugal pump by using a numerical simulation, Kriging model (KRG), Latin hypercube design and GA. Wang et al. [9] coupled the MGA NSGA- II and back propagation neural network to enhance a NASA rotor37. Bing et al. [10] optimized the mixed-flow pump impeller based on the GA and the iterative design

*Corresponding author. Tel.: +86 51188786770, Fax.: +86 511 88790358
E-mail address: jpei@ujs.edu.cn
† This paper was presented at the ISFMFE 2014, Wuhan, China, October 2014. Recommended by Guest Editor Hyung Hee Cho and Yulin Wu

Table 1. Main parameters of the pump.

Impeller	Value	Diffuser	Value	Volute	Value
D_j/ mm	270	D_3/ mm	515	D_5/ mm	840
D_2/mm	511	D_4/ mm	718	b_5/ mm	250
b_2/ mm	49	b_3/ mm	55	n_s	105
Z_i	5	b_4/ mm	84	n/ r min^{-1}	1490
		Z_d	7	η	76%

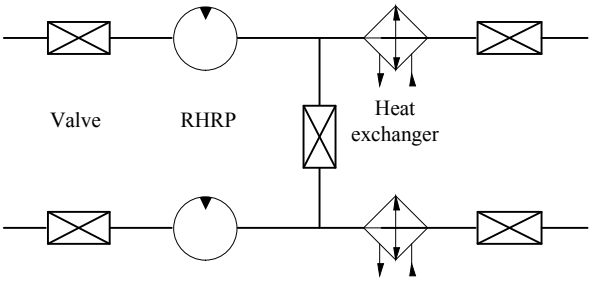

Fig. 1. Residual heat removal system.

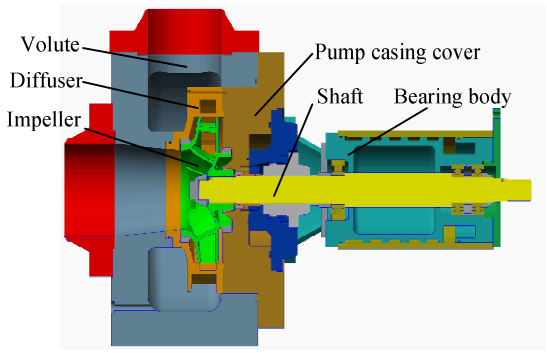

(a) Axial section of residual heat removal pump

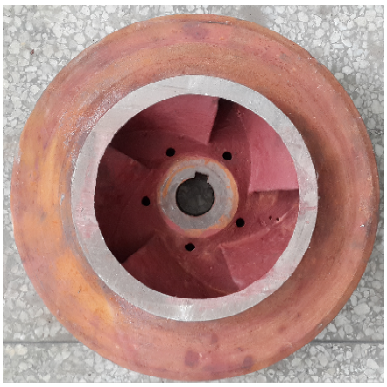

(b) Schematic profile of model impeller

Fig. 2. Residual heat removal pump model.

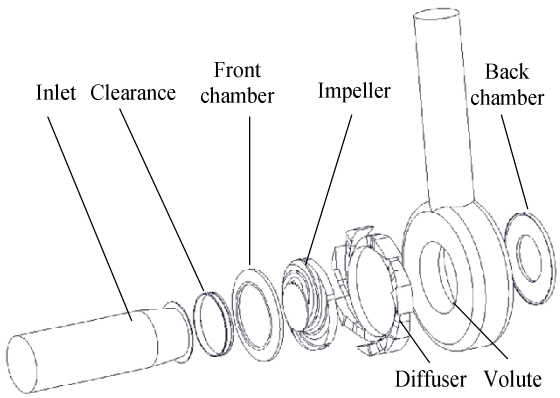

Fig. 3. Whole computational domain.

method of the direct and inverse problems. The optimization strategy improved the hydraulic efficiency of the impeller, which increased by 3%. Kim et al. [11] suggested an optimization process that was based on a Radial basis neural network (RBNN) model and Sequential quadratic programming (SQP) to seek the best combination of diffuser parameters for improving the performance of the mixed flow pump. Kim et al. [12] carried out a numerical optimization coupling surrogated model and SQP to improve the performance of a tunnel ventilation jet fan. He also applied factorial design to optimize the pump impeller with the response surface method [13].

In this paper, an optimization method is proposed by combining the design of experiment, surrogate model, GA, and CFD analysis. Latin hypercube sampling (LHS) method is applied to design the sampling points of the impeller. A suitable surrogate model is selected by comparing three surrogate models constructed by CFD results. Finally, GA is applied to seek the best parameters of impeller to maximize the efficiency under the design point.

2. Geometry

The hydraulic components of a centrifugal pump include a twist impeller with five blades, radial diffuser with seven vanes, and an annular volute. The design flow rate Q and head H of the pump are 910 m^3/h and 77 m, respectively. The specific geometric parameters of the pump are shown in Table 1. Fig. 2 shows that the structure type of pump is horizontal, single-stage, and with a single suction. Fig. 3 illustrates that the whole computational domain consists of seven parts, namely, inlet, impeller, diffuser, front chamber, back chamber, clearance of wearing ring, and volute. To prevent the backflow from extending to the whole inlet pipe and the recirculation at the outlet pipe, the length of inlet pipe and outlet pipe added to the volute is extended.

3. Numerical simulation and experimental validation

3.1 Mesh generation

Mesh generation is an important step in the process of numerical simulation by directly affecting the accuracy and calculation time. The structured grids of the whole computational domain are generated by the meshing tool ICEM. The mesh of the main domain is shown in Fig. 4. The mesh independence check was performed in a previous research [14]. Fig. 5 shows that when the grid number increases from 5.49 million to 6.01

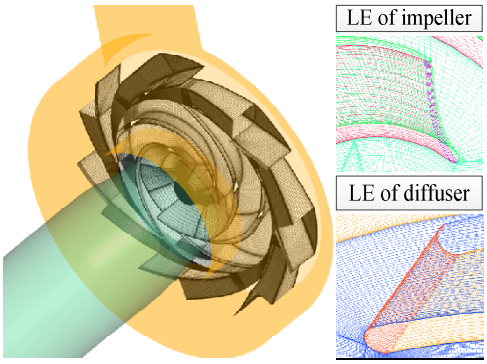

Fig. 4. Mesh of impeller and diffuser.

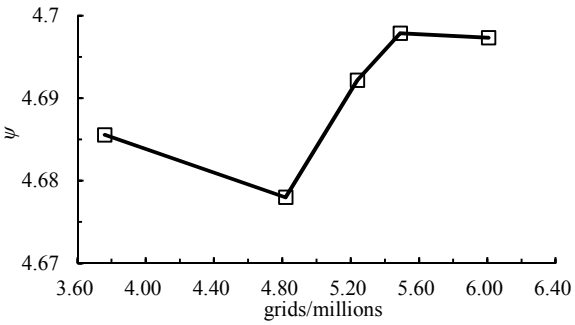

Fig. 5. Mesh independence analysis.

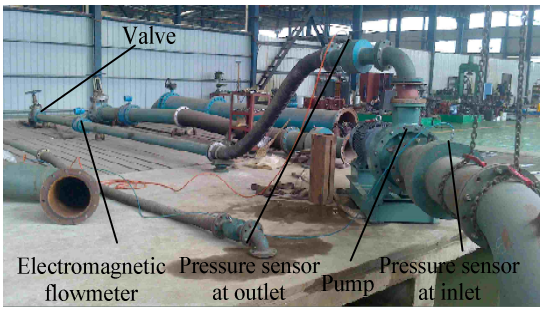

Fig. 6. Open test rig.

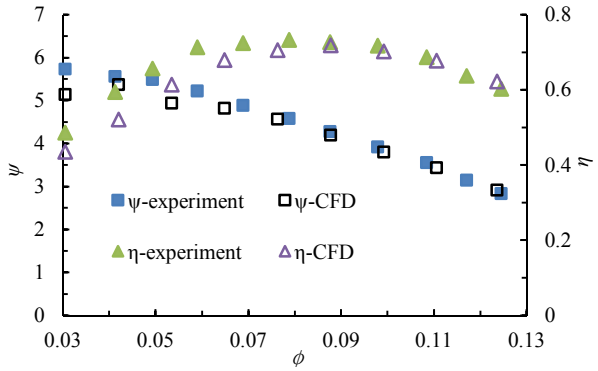

Fig. 7. Comparison between CFD and experimental results.

million, the head remains stable. Finally, approximately 5.5 million grids are determined to carry out the numerical simulation.

3.2 Mesh generation

The 3D steady numerical simulation is performed by using ANSYS CFX 14.5 when the fluid in the pump is supposed to be incompressible and viscous. The Reynolds-averaged Navier-Stokes is solved with the Shear stress transport (SST) *k-ω* turbulence model, which is derived by Menter [15]. The SST *k-ω* model accounts for the transport of the turbulent shear stress and gives highly accurate predictions of the onset and amount of flow separation under adverse pressure gradients by the inclusion of effects into the formulation of the eddy viscosity. This turbulence model is a blending between the *k-ω* model near the surface and the *k-ε* model in the outer region.

Multi-reference frame technique is used in the steady simulation. 'Frozen rotor' is set in the interface between the rotor and stator, while 'None' is set in the stator–stator interface. The boundaries at the inlet and outlet are specified by total pressure and mass flow rate respectively. According to the actual roughness on the walls of hydraulic components, the solid walls on the impeller blades and diffuser vanes are considered to be rough, with a roughness of 6.3 μm, while the roughness of other walls is 12.5 μm. The surfaces in the whole computational domains are no-slip conditions. The physical time scale is $1/\omega$ and ω is the angular velocity of the pump. The root mean square residual value is set below 10^{-5}. The numerical calculation is performed on a Dell Workstation T3600 with an Intel Xeon CPU E5-1650 and a clock speed of 3.2 GHz.

3.3 Experimental validation

The accuracy validation of the numerical simulation for performance prediction is critical before the optimization of the impeller blade can be processed. Fig. 6 shows the original model pump (scaled to 0.7 times of the real pump) was tested in the open test rig of Yixing Unite Machinery Co. Ltd. Fig. 7 presents the comparison of performance between numerical and experimental results. The predicted performance agrees with the experimental results. Thus, the numerical simulation can accurately and reliably predict the performance of the pump. The efficiency calculated by CFD is 70.57%, while the experimental efficiency is 73.3% with a relative error of 3.9%. The flow coefficient ϕ and head coefficient ψ are defined as follows:

$$\phi = \frac{Q}{nD_2^3}. \tag{1}$$

$$\psi = \frac{gH}{n^2 D_2^2}. \tag{2}$$

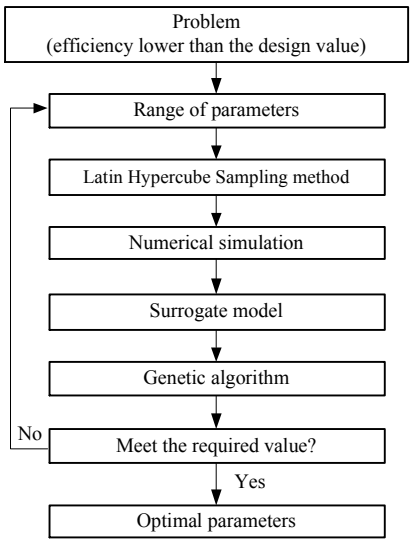

Fig. 8. Flow chart of optimization.

4. Optimization process

The pump efficiency (73.3%) cannot meet the required value of 76%, and thus optimizing the impeller is necessary. The optimization process is illustrated in the flow chart in Fig. 8. First, the initial values of the design variables are determined, and the efficiency under the design point is selected as the objective. Second, the design space points are chosen by using the LHS method. The objectives at these design points are calculated by numerical simulation. Three surrogate models are built between the objectives and the design variables. Then the prediction accuracy of three surrogate models are compared. Finally, the selected optimal combination of design parameters is explored by solving the suitable surrogate model with the Multi-island genetic algorithm (MIGA). During the optimization process, the computational domain of the impeller is constructed by the software CFturbo, the mesh is generated by ICEM, the steady simulation is executed by CFX, and the surrogate model and GA are combined to obtain the optimal parameters based on the Isight 5.7 software.

4.1 Objective function

The optimization aims to maximize the efficiency η. The equation is as follows:

$$\eta = \frac{\rho g Q H}{P} . \tag{3}$$

4.2 Design parameters

To keep the impeller safe, the thickness of the impeller is unchanged. The profile of the blade is optimized, and the three parameters are the inlet incidence angle $\Delta\beta$, blade wrap angle φ, and blade outlet angle β_2. The inlet incidence angle $\Delta\beta$ is defined as

Table 2. Ranges of blade parameters.

Parameters	Lower value	Upper value	Original value
$\Delta\beta$	5°	9°	9°
φ	120°	150°	115°
β_2	20°	24°	23°

Table 3. Efficiencies under 16 design points.

No.	β_2/°	$\Delta\beta$/°	φ/°	η/%
1	20	9	146	75.72
2	20.27	5.8	126	75.43
3	20.53	7.93	150	75.94
4	20.8	6.33	128	75.49
5	21.07	5.53	120	74.94
6	21.33	6.6	132	75.70
7	21.6	5.27	134	74.98
8	21.87	5	144	76.19
9	22.13	6.87	136	75.36
10	22.4	7.13	142	75.82
11	22.67	8.73	124	74.60
12	22.93	8.47	130	74.25
13	23.2	7.67	138	74.79
14	23.47	7.4	140	74.96
15	23.73	6.07	148	75.48
16	24	8.2	122	73.64

$$\Delta\beta = \beta_1 - \beta_1^{'} . \tag{4}$$

where β_1 and β_1' are the blade inlet angle and inlet flow angle respectively. β_1' can be calculated by the velocity triangle.

According to the design method of the pump [16] and a previous investigation of the optimization on the impeller [17], the ranges of the design parameters are determined, as shown in Table 2.

4.3 Latin hypercube sampling method

The design of experiment is widely used to perform the optimization, such as the Taguchi method, factorial design, LHS, and so on. The advantage of the Taguchi method and uniform design is that they obtain less experimental programs to yield the best results; its disadvantage is that the best combination of parameters cannot be easily found. The LHS method can randomly generate a range of parameters that represent all proportions of the design space. A total of 16 schemes are designed by the LHS method, and the results under the design point at every design point are calculated, as shown in Table 3.

4.4 Surrogate models

The surrogate model [18-20], similar to the response surface method, KRG, RBNN, and so on, can reduce the numerical

calculation time to a certain extent. The best combination of parameters can be obtained by solving the function with the optimization algorithm. Establishing the surrogate model is a key step for optimization accuracy. Several types of surrogate models are briefly introduced as follows.

4.4.1 Response surface approximation (RSF)

RSF is a method that studies the quantitative relationship between the objective function $f(x)$ and the variable x.

$$f(x) = \sum b_i f_i(x) \ . \tag{5}$$

where $f_i(x)$ is the basic function. The coefficient b_i is calculated by minimizing the relative error between the objective function $f(x)$ and the real values $y(x)$, which is obtained from the experiments or numerical simulations.

The coefficient b_i is as follows:

$$b = (x^T x)^{-1} x^T y \ . \tag{6}$$

4.4.2 Kriging model (KRG)

KRG is made up of a regression function and a random function.

$$f(x) = \sum b_i f_i(x) + z(x) \ . \tag{7}$$

The random function $z(x)$ is supposed to have a mean zero and covariance.

$$E\left[z(x), z(y)\right] = \sigma^2 r(\theta, x, y) \ . \tag{8}$$

where $r(\theta, x, y)$ is the correlation model with parameters θ. In this paper, the correlation model is selected as the GAUSS function.

$$r(\theta, x, y) = \prod_{j=1}^{n} \exp(-\theta_j (x_j - y_j)^2) \ . \tag{9}$$

4.4.3 Radial basis neural network (RBNN)

The RBNN model is built as a weighted combination of responses from radial basis functions.

$$f(x) = \sum w_i f_i(x) \ . \tag{10}$$

where $f_i(x)$ is the response of the radial basis function and w_i is the weight of the $f_i(x)$. The GAUSS function is used for the radial basis function.

5. Results and discussion

5.1 Comparison of prediction accuracy

Evaluating the accuracy of surrogate models is necessary. Thus, the error analysis method of R-square is used to evaluate the prediction accuracy of surrogate models. If the R-square value is more than 0.9, then the surrogate model has good prediction capability. Fig. 9 shows that the values of RSF, KRG, and BPNN are 0.9387, 0.993 and 1, respectively, which means that the three surrogate models have good capabilities in predicting the efficiency, with the KRG and BPNN having better prediction accuracy.

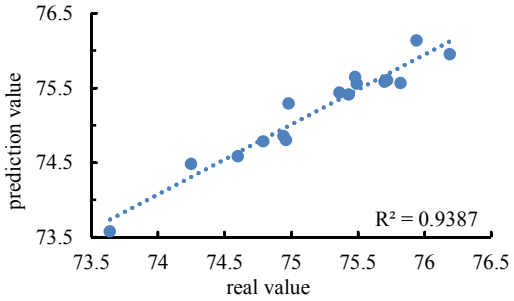

(a) Response surface method

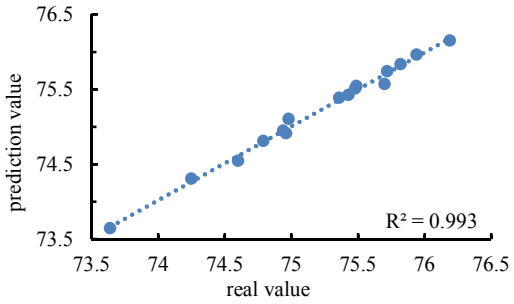

(b) Kriging model

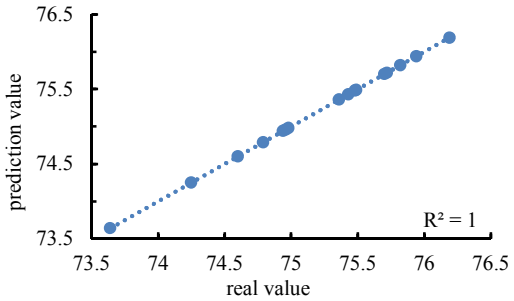

(c) Radial basis neural network

Fig. 9. Prediction accuracy of surrogate models.

5.2 Comparison of optimization result

After the establishment of the surrogate model is completed, the optimization algorithm is applied to seek the best combination of designed parameters of the impeller by solving the surrogate model. The optimization algorithm is divided into the direct search algorithm and global search algorithm. The advantage of direct search algorithms, like the Hooke-Jeeves direct search method and downhill simplex, is their effectiveness in seeking the local area of the initial design points. However, they may not find the best combination of parameters. In contrast, global search algorithms such as GA, particle

Table 4. Settings of the MIGA.

Parameters	Value
Sub-population	10
Number of islands	10
Number of generations	50
Rate of crossover	0.9
Rate of mutation	0.01
Rate of migration	0.01
Interval of migration	5
Elite size	1

Table 5. Comparison of parameters and results.

Surrogate model	β_2/°	$\Delta\beta$/°	φ/°	η/% prediction	η/% CFD	Relative error
RSF	20.6	5.7	150	76.65	76.45	0.26%
KRG	21.5	5.9	148	76.49	76.37	0.17%
RBNN	21.3	5.2	150	76.26	76.26	0.005%

swarm optimization, and adaptive simulated annealing, are better for surrogate functions, which are nonlinear, non-differentiable, and discontinued, though the calculation costs more computational source and time. These are applied to solve complex engineering problems [21-23]. In this paper, the MIGA is developed from the traditional GA and has better global search ability. Detailed settings of the MIGA are shown in Table 4. The optimization calculation executes 5000 iterations.

The best combination of parameters is obtained by solving the surrogate model with MIGA. Optimal parameters acquired from three surrogate models are shown in Table 5. The efficiency predicted by the RSM is shown to be the highest (76.65%), followed by those of the KRG and RBNN.

According to the parameters of the three surrogate models, the impellers are rebuilt by CFturbo and the same numerical simulation settings are carried out at the CFX 14.5 platform. The comparison of efficiencies between the numerical simulation and prediction by surrogate models are illustrated in Table 5. The RBNN has the highest prediction accuracy, while its calculated efficiency is the lowest. The efficiency predicted by RSF is the highest and the relative error is ranked third. Compared with the simulated efficiency (70.57%) of the original pump, the optimization increases the efficiency by 8.34%. Thus, the final optimal parameters of the impeller are obtained by calculating RSF with MIGA.

5.3 Comparison of flow field

Fig. 10 shows the pressure distribution on blades at 50% span of the impeller along the streamline from the leading edge to the trailing edge. The pressure distribution of the optimal impeller is more regular than that of the original one, whose lowest pressure occurs at 0.05 of the streamline location at the suction side. The pressure is larger on the suction side of the optimal blades and smaller on the pressure side below 0.5 of the streamline location. The pressure on the blades is almost the same between 0.5 and 0.8 of streamline location. The distribution of pressure at the trailing edge is complex due to the jet-wake flow.

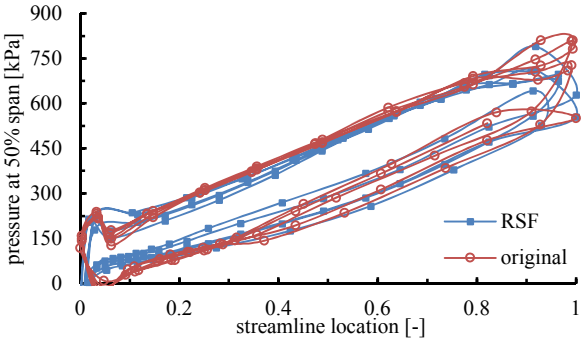

Fig. 10. Pressure distribution on blades at 50% span.

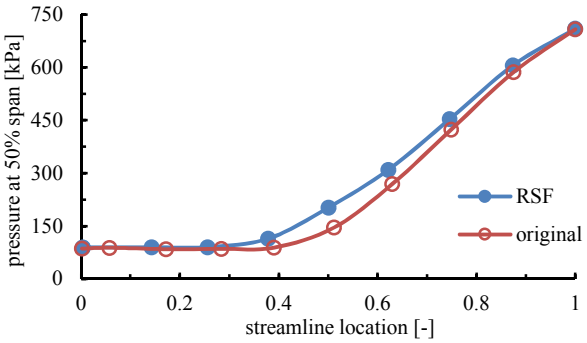

Fig. 11. Pressure distribution from inlet to outlet.

The pressure distribution from inlet to outlet is shown in Fig. 11. When the streamline is approximately below 0.3, the pressure is constant. In the original impeller, the pressure reaches its lowest at 0.4 of the streamline location and then slowly increases to 0.4 of the streamline location. The pressure then increases faster in the original impeller than that in the optimal one. Thus, the hydraulic loss in the original impeller is larger.

The relative velocity vectors at 50% span of the original and optimal impellers are compared, as presented in Fig. 12. Flow separation occurs at the pressure side of both impellers. In the original impeller, a low velocity area exists at the suction side of blade, while fluid flows along the suction side of the optimal blade regularly. Thus, the optimal impeller passage has good flow control and less hydraulic loss is generated.

6. Conclusions

An optimization process of the impeller is applied to improve the efficiency of an RHRP. The optimization strategy is proposed based on numerical simulation, design of experiment, surrogate model, and GA. Three surrogate models, namely, RSM, KRG, and RBNN, are compared during the construc-

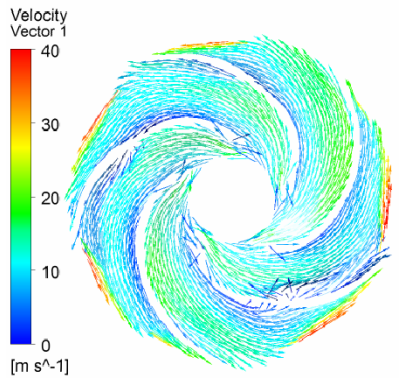

(a) Original impeller

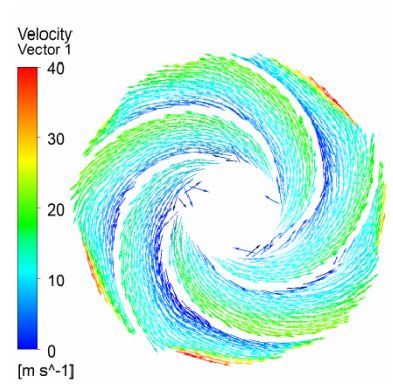

(b) Optimal impeller

Fig. 12. Velocity vectors at 50% span of impeller.

tion of the best surrogate model between the efficiency and the impeller parameters. The RSF model predicts the highest efficiency, whereas the RBNN has the highest prediction accuracy. Finally, the optimization increases the efficiency of the pump by 8.34%. Compared with the inner flow field of the original impeller, the pressure distributions on the optimum blades are more regular and the area of flow separation disappears at the suction side near the trailing edge. The optimization process, including the comparison of the different surrogate models, can provide reference for the optimal design of other pumps.

Acknowledgment

This work is supported by the National Natural Science Foundation of China (Grant No. 51409123), Natural Science Foundation of Jiangsu Province (Grant No. BK20140554), China Postdoctoral Science Foundation (Grant No. 2015T 80507), Postdoctoral Science Foundation of Jiangsu Province (Grant No. 1401069B), and Innovation Project for Postgraduates of Jiangsu Province (Grant No. KYLX15_1066).

Nomenclature

b_2 : Impeller blade outlet width
b_3 : Diffuser vane inlet width
b_4 : Diffuser vane outlet width
b_5 : Volute inlet width
D_j : Impeller inlet diameter
D_2 : Impeller outlet diameter
D_3 : Diffuser inlet diameter
D_4 : Diffuser outlet diameter
D_5 : Volute inlet diameter
g : Acceleration of gravity
H : Head
LE : Leading edge
n : Rotating speed
n_s : $3.65\times nQ^{0.5}/H^{0.75}$, specific speed
P : Power
Q : Flow rate
Z_i : Number of blade
Z_d : Number of vane
β_1 : Blade inlet angle
β_2 : Blade outlet angle
β_1' : Inlet flow angle
$\Delta\beta$: Blade inlet incidence angle
η : Efficiency
ρ : Density
φ : Blade wrap angle
ϕ : Flow coefficient
ψ : Head coefficient

References

[1] P. Liu, X. Long and H. Guan, Discussion about residual heat removal pump in nuclear power plant, *Pump Technology*, 6 (2008) 18-20.

[2] R. R. Singh and M. Nataraj, Analysis and optimization of pump performance variables using genetic algorithm and taguchi quality concept: A case study, *International Journal of Mechanical Engineering application Research*, 3 (3) (2012) 185-189.

[3] L. Zhou, W. Shi and S. Wu, Performance optimization in a centrifugal pump impeller by orthogonal experiment and numerical simulation, *Advances in Mechanical Engineering*, 2013 (2013).

[4] Y. Lian and M. Liou, Multiobjective optimization using coupled response surface model and evolutionary algorithm, *AIAA Journal*, 43 (6) (2005)1316-1325.

[5] W. Yang and R. Xiao, Multiobjective optimization design of a pump–turbine impeller based on an inverse design using a combination optimization strategy, *Journal of Fluids Engineering*, 136 (1) (2014) 014501.

[6] C. Wang, H. Peng, J. Ding and D. Liu, Optimization for s-type blade of fire pump based on response surface method, *Journal of Mechanical Engineering*, 49 (10) (2013) 170-177.

[7] R. Zhang, K. Zheng and J. Yang, Investigation on parametric design of centrifugal pump impeller and its optimization with response surface method, *ASME 2012 Fluids Engineering Division Summer Meeting collocated with the ASME*

2012 Heat Transfer Summer Conference and the ASME 2012 10th International Conference on Nanochannels, Microchannels, and Minichannels, American Society of Mechanical Engineers (2012) 529-533.

[8] Y. Zhang, S. Hu, J. Wu, Y. Zhang and L. Chen, Multi-objective optimization of double suction centrifugal pump using Kriging metamodels, *Advances in Engineering Software*, 74 (2014)16-26.

[9] X. Wang, C. Hirsch, S. Kang and C. Lacor, Multi-objective optimization of turbomachinery using improved NSGA-II and approximation model, *Computer Methods in Applied Mechanics and Engineering*, 200 (9) (2011) 883-895.

[10] H. Bing and S. Cao, Optimal design of mixed-flow pump impeller based on direct inverse problem iteration and genetic algorithm, *ASME-JSME-KSME 2011 Joint Fluids Engineering Conference,* American Society of Mechanical Engineers (2011) 803-810.

[11] J. H. Kim and K. Y. Kim, Analysis and optimization of a vaned diffuser in a mixed flow pump to improve hydrodynamic performance, *Journal of Fluids Engineering*, 134 (7) (2012) 071104.

[12] J. H. Kim, J. H. Kim, K. Y. Kim, J. Y. Yoon, S. H. Yang and Y. S. Choi, High-efficiency design of a tunnel ventilation jet fan through numerical optimization techniques, *Journal of Mechanical Science and Technology*, 26 (6) (2012) 1793-1800.

[13] J. H. Kim, H. C. Lee, J. H. Kim, S. Kim, J. Y. Yoon and Y. S. Choi, Design techniques to improve the performance of a centrifugal pump using CFD, *Journal of Mechanical Science and Technology*, 29 (1) (2015) 215-225.

[14] J. Pei, S. Yuan and W. Wang, Numerical analysis of three-dimensional unsteady turbulent flow in circular casing of a high power centrifugal diffuser pump, *Advances in Mechanical Engineering* (2013).

[15] F. R. Menter, Two-equation eddy viscosity models for engineering applications, *AIAA Journal*, 32 (8) (1994) 1598-1605.

[16] X. Guan, *Modern pumps theory and design*, First Ed., China Astronautic Publishing House, Beijing, China (2011).

[17] W. Wang, S. Yuan, J. Pei, J. Zhang, J. Yuan and J. Mao, Optimum hydraulic design for a radial diffuser pump using orthogonal experimental method based on *CFD*, *ASME 2014 4th Joint US-European Fluids Engineering Division Summer Meeting collocated with the ASME 2014 12th International Conference on Nanochannels, Microchannels, and Minichannels,* American Society of Mechanical Engineers (2014) V01AT02A002-V01AT02A002.

[18] T. Goel, D. J. Dorney, R. T. Haftka and W. Shyy, Improving the hydrodynamic performance of diffuser vanes via shape optimization, *Computers & Fluids*, 37 (6) (2008) 705-723.

[19] T. Goel, R. Vaidyanathan, R. T. Haftka, W. Shyy, N. V. Queipo and K. Tucker, Response surface approximation of Pareto optimal front in multi-objective optimization, *Computer Methods in Applied mechanics and Engineering*, 196 (4) (2007) 879-893.

[20] N. V. Queipo, R. T. Haftka, W. Shyy, T. Goel, R. Vaidyanathan and K. Tucker, Surrogate-based analysis and optimization, *Progress in Aerospace Sciences*, 41 (1) (2005) 1-28.

[21] S. Derakhshan, B. Mohammadi and A. Nourbakhsh, The comparison of incomplete sensitivities and Genetic algorithms applications in 3D radial turbomachinery blade optimization, *Computers & Fluids*, 39 (10) (2010) 2022-2029.

[22] X. Yuan, T. Tanuma, X. Zhu, Z. Lin and D. Nomura, A CFD approach to fluid dynamic optimum design of steam turbine stages with stator and rotor blades, *ASME Turbo Expo 2010: Power for Land, Sea, and Air,* American Society of Mechanical Engineers (2010) 2209-2218.

[23] I. Tsalicoglou and B. Phillipsen, Design of radial turbine meridional profiles using particle swarm optimization, *2nd International Conference on Engineering Optimization* (2010).

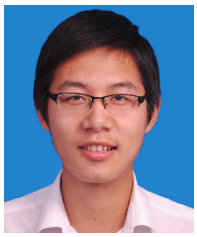

Wenjie Wang is currently a Ph.D. candidate in the National Research Center of Pumps, Jiangsu University. His research interests include the optimization design and analysis of unsteady flow of centrifugal pump. He received his B.S. degree from Jiangsu University in 2008.

Ji Pei is currently an assistant professor in the National Research Center of Pumps, Jiangsu University. His research interests include unsteady flow, flow-induced vibration, and fluid-structure interaction in turbomachinery. He received his Ph.D. degree from Jiangsu University in 2013.

Shouqi Yuan is currently a professor in the National Research Center of Pumps, Jiangsu University. His research interests include the theory, optimization, and design of fluid machinery. He received his Ph.D. degree from Jiangsu University in 1994.